

**Supporting information for**  
**Selective construction and stability studies of molecular trefoil**  
**knot and Solomon link**

Li-Long Dang,<sup>\*a</sup> Ting-Ting Li,<sup>a,c</sup> Zheng Cui,<sup>b</sup> Dong Sui,<sup>a</sup> Lu-Fang Ma<sup>a</sup> and Guo-Xin Jin<sup>\*b</sup>

a.College of Chemistry and Chemical Engineering Henan Province Function-Oriented Porous Materials Key Laboratory, Luoyang Normal University, Luoyang 471934, P. R. China

b.Shanghai Key Laboratory of Molecular Catalysis and Innovative Materials, State Key Laboratory of Molecular Engineering of Polymers, Department of Chemistry, Fudan University, Shanghai 200438, P. R. China

c.College of Chemistry and Bioengineering (Guangxi Key Laboratory of, Electrochemical and Magnetochemical Functional Materials), Guilin University of Technology, Guilin 541004, People's Republic of China

\*E-mail: danglilong8@163.com; gxjin@fudan.edu.cn

**Contents**

- 1. General considerations**
- 2. Synthesis of ligand L1, complex 1 and 3**
- 3. Single-crystal X-ray structure of 1 and 3**
- 4. NMR spectra**
- 5. UV-vis-NIR absorption spectra**
- 6. ESI-MS spectra**
- 7. DFT computational details**
- 8. X-ray crystallography details**
- 9. References**

## 1. General considerations

All reagents and solvents were purchased from commercial sources and used as supplied unless otherwise mentioned. The starting materials  $[\text{Cp}^*\text{RhCl}_2]_2$  ( $\text{Cp}^* = \eta^5\text{-pentamethylcyclopentadienyl}$ )<sup>[1]</sup>,  $[\text{Cp}^*_2\text{Rh}_2(\text{L2})](\text{OTf})_2$  (**E1**),  $[\text{Cp}^*_2\text{Rh}_2(\text{L3})](\text{OTf})_2$  (**E2**) and ligand **L1** were prepared by literature methods. NMR spectra were recorded on Bruker AVANCE I 400 spectrometers at room temperature and referenced to the residual protonated solvent. Proton chemical shifts are reported relative to the solvent residual peak ( $\delta$  H = 3.31 ( $\text{CD}_3\text{OD}$ ), 2.50 ( $\text{DMSO-D6}$ ), 1.94 ( $\text{CD}_3\text{CN}$ ), 2.75, 2.92 ( $\text{DMF}$ )) and  $\delta$  C = 49.00 ( $\text{CD}_3\text{OD}$ ), 29.76, 34.89 ( $\text{DMF}$ ). Coupling constants are expressed in Hertz. Elemental analyses were performed on an Elementar Vario EL III analyzer. ESI-MS spectra were recorded on a Micro TOF II mass spectrometer.

## 2. Synthesis of ligand L1, complex 1 and 3

**Synthesis of N, N'-bis(3-pyridylmethyl)-diphthalic diimide (L1):** A mixture of diphthalic dianhydride (3.1 g, 10 mmol) and 3-aminomethyl-pyridine (2.2 g, 21 mmol) in DMF (40 mL) was heated to reflux with stirring for 5 h. On cooling of the sample, the yellow solution was filtered, and the off-white crude solid was collected and washed with cold DMF. A white powder was obtained by recrystallization of the solid from DMF. Yield: 85%. Anal. calcd. for  $\text{C}_{28}\text{H}_{18}\text{O}_4\text{N}_4$ : C, 70.88; H, 3.82; N, 11.81. Found: C, 70.96; H, 3.78; N, 11.86%. <sup>1</sup>H NMR (ppm, **DMSO-D6**)  $\delta$ : 8.60 (d, J = 1.6 Hz, 2H), 8.50 (d, J = 5.2 Hz, 2H), 8.33 (s, 2H), 8.30 (d, J = 8 Hz, 2H), 8.02 (d, J = 8 Hz, 2H), 7.75 (d, J = 7.6 Hz, 2H), 7.39-7.35 (m, 2H), 4.85 (s, 2H).

### Synthesis of complex 1 (Trefoil knot)

$\text{AgOTf}$  (123.2 mg, 0.48 mmol) was added to a solution of  $[\text{Cp}^*\text{RhCl}_2]_2$  (74.4 mg, 0.12 mmol) in  $\text{CH}_3\text{OH}$  (20 mL) at room temperature. The reaction mixture was stirred in the dark for 12 h and then filtered. 6,11-Dihydroxy-5,12-naphthacene dione (**L2**) (34.8 mg, 0.12 mmol) and NaOH (9.6 mg, 0.24 mmol) was added to the filtrate. The mixture was stirred at room temperature for 12 h to give a dark green solution. **L1** (56.88 mg, 0.12 mmol) was then added. The mixture was stirred at room temperature for another 12 h to give a dark green solution. The solvent was concentrated to about 8 mL. Upon addition of diethyl ether, a dark green solid was precipitated and collected. The product was recrystallized from a methanol/diethyl ether mixture to afford block-shaped crystals (**1**). 73.90 mg, yield 86.5%. Anal. Calcd for  $\text{C}_{204}\text{H}_{168}\text{O}_{42}\text{N}_{12}\text{S}_6\text{F}_{18}\text{Rh}_6$  (M = 4611.39): C, 53.13; H, 3.67; N, 3.64. Found: C, 53.16; H, 3.63; N, 3.67. <sup>1</sup>H NMR (500 MHz,  $\text{CD}_3\text{OD}$ , ppm, with respect to  $\text{Cp}^*\text{Rh}$ ):  $\delta$  = 9.27 (s, 6H, phenyl-H of L1),  $\delta$  = 9.19 (d, J = 3.6, 6H, pyridyl-H),  $\delta$  = 8.74 (d, J = 6.0, 6H, L2- $\alpha$ H),  $\delta$  = 8.27 (d, J = 6.0, 6H, pyridyl-H),  $\delta$  = 8.17 (d, J = 4.4, 6H, pyridyl-H),  $\delta$  = 7.85 (t, 6H, pyridyl- $\beta$ H),  $\delta$  = 7.73 (d, J = 6.4, 6H, L2- $\alpha$ H),  $\delta$  = 7.57 (t, 6H, L2- $\beta$ H),  $\delta$  = 6.20 (s, 6H, pyridyl-H),  $\delta$  = 5.53 (d, J = 5.6, 6H, - $\text{CH}_2$ -),  $\delta$  = 5.15-5.08 (m, 12H, phenyl-H of L1),  $\delta$  = 3.93 (d, J = 6.0, 6H, - $\text{CH}_2$ -),  $\delta$  = 1.46 (s, 90H,  $\text{Cp}^*$ ).  $\delta$  = <sup>13</sup>C{<sup>1</sup>H} (101 MHz,  $\text{CD}_3\text{OD}$ , ppm):  $\delta$  = 8.42 ( $\text{Cp}^*$ ), 39.53, 49.00, 95.52, 111.52, 120.32, 120.45, 122.27, 123.48, 127.19, 128.45, 129.72, 129.75, 131.25, 134.33, 137.12, 137.39, 141.07, 142.55, 153.34, 153.86, 166.58, 167.62, 171.92, 173.19. IR (KBr disk,  $\text{cm}^{-1}$ ):  $\nu$  = 3857, 3736, 3585, 3563, 1769, 1715, 1546, 1449, 1388, 1267, 1158, 1068, 1043, 1031, 928, 741, 704, 698, 639, 578, 512. ESI-MS: m/z 2155.23 (calcd for  $[\text{M} - 2\text{OTf}]^{2+}$  2155.23).

### Synthesis of complex 2 ([2+2] macrocycle)

$\text{AgOTf}$  (123.2 mg, 0.48 mmol) was added to a solution of  $[\text{Cp}^*\text{RhCl}_2]_2$  (74.4 mg, 0.12 mmol) in the

mixture solution of CH<sub>3</sub>OH (4 mL) and DMF (16 mL) at room temperature. The reaction mixture was stirred in the dark for 12 h and then filtered. 6,11-Dihydroxy-5,12-naphthacene dione (**L2**) (34.8 mg, 0.12 mmol) and NaOH (9.6 mg, 0.24 mmol) was added to the filtrate. The mixture was stirred at room temperature for 12 h to give a dark green solution. **L1** (56.88 mg, 0.12 mmol) was then added. The mixture was stirred at room temperature for another 12 h to give a dark green solution. The solvent was concentrated to about 8 mL. Upon addition of diethyl ether, a dark green solid was precipitated and collected. The product was recrystallized from a methanol/diethyl ether mixture to afford block-shaped crystals (**2**). 151.25 mg, yield 82.0%. Anal. Calcd for C<sub>136</sub>H<sub>112</sub>O<sub>28</sub>N<sub>8</sub>S<sub>4</sub>F<sub>12</sub>Rh<sub>4</sub> (M = 3072.25): C, 53.13; H, 3.67; N, 3.64. Found: C, 53.17; H, 3.62; N, 3.68. <sup>1</sup>H NMR (500 MHz, CD<sub>3</sub>OD, ppm, with respect to Cp\*Rh): δ = 8.819 (d, J=1.5, 2H, pyridyl-H), 8.709 (s, 2H, PDM-H), 8.632 (d, J=5.5, 2H, PDM-H), 8.207 (d, J=8, 2H, PDM-H), 8.070 (s, 2H, pyridyl-H), 7.857 (d, J=6, 2H, L2-H), 7.809 (d, J=7, 2H, L2-H), 7.454 (t, 2H, pyridyl-H), 4.970 (s, 4H, -CH<sub>2</sub>-), 1.758 (s, 30H, Cp\*-H).

### Synthesis of complex 3 (Solomon link)

AgOTf (123.2 mg, 0.48 mmol) was added to a solution of [Cp\*RhCl<sub>2</sub>]<sub>2</sub> (74.4 mg, 0.12 mmol) in CH<sub>3</sub>OH (20 mL) at room temperature. The reaction mixture was stirred in the dark for 12 h and then filtered. H<sub>2</sub>DPPP (**L3**) (34.8 mg, 0.12 mmol) and NaOH (9.6 mg, 0.24 mmol) was added to the filtrate. The mixture was stirred at room temperature for 12 h to give a dark green solution. **L1** (56.88 mg, 0.12 mmol) was then added. The mixture was stirred at room temperature for another 12 h to give a dark green solution. The solvent was concentrated to about 8 mL with a rotary evaporator. On addition of diethyl ether, the respective Solomon link precipitated and were collected and dried under vacuum. The product was recrystallized from a methanol/diethyl ether mixture to afford block-shaped crystals (**3**). 158.9 mg, yield 86.2%. Anal. Calcd for C<sub>264</sub>H<sub>224</sub>N<sub>32</sub>O<sub>48</sub>S<sub>8</sub>F<sub>24</sub>Rh<sub>8</sub> (M = 5784.38): C, 54.82; H, 3.90; N, 1.45. Found: C, 54.85; H, 3.93; N, 1.41. <sup>1</sup>H NMR (500 MHz, CD<sub>3</sub>OD, ppm, with respect to Cp\*Rh, see Fig. S15): δ = 9.27 (d, J = 7.0, 8H, pyridyl-Hi of E2), δ = 8.98 (t, J = 6.5, 8H, pyridyl-Hi of E2), δ = 8.51-8.48 (m, 16H, pyridyl-Hb and Hc of L1), δ = 8.42-8.37 (m, 8H, pyridyl-Hj of E2), δ = 8.18-8.12 (dd, J = 9.5, 8H, PDM-Hf of L1), δ = 8.03-7.98 (m, 16H, pyridyl-Hk of E2 and pyridyl-Ha of L1), δ = 7.90-7.85 (m, J = 8.5, 8H, pyridyl-Hd of L1), δ = 7.78 (d, J = 10.0, 8H, PDM-Hg of L1), δ = 7.38-7.34 (m, 8H, pyridyl-Hc of L1), δ = 4.56-4.42 (m, 16H, -CH<sub>2</sub>-), δ = 1.71 (d, J = 4.5, 120H, Cp\*-Hm). IR (KBr disk, cm<sup>-1</sup>): ν = 3854, 3823, 3807, 3755, 3737, 3670, 3633, 3587, 3568, 1773, 1716, 1616, 1462, 1392, 1348, 1275, 1251, 1225, 1158, 1100, 1030, 826, 786, 746, 635, 575, 515. ESI-MS: m/z 1899.24 (calcd for [M - 3OTf]<sup>3+</sup> 1899.24).

### 3. Single-crystal X-ray structure of complex 1 and 3

### 3.1 Single-crystal X-ray structure of complex 1

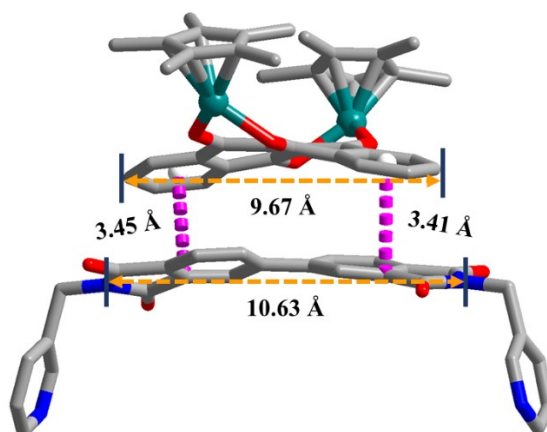


**Fig. S1.** Partial presentation of single-crystal X-ray structure of **1**,  $\pi$ - $\pi$  stacking interactions between the phthalic diimide moieties of **L1** and benzene rings of the **L2** moieties of **E1**. C-H $\cdots$  $\pi$  interactions between protons of benzene rings of **L1** and **L2** moiety. (N, blue; O, red; C, gray; Rh, green; H, rose).

### 3.2 Single-crystal X-ray structure of complex 3

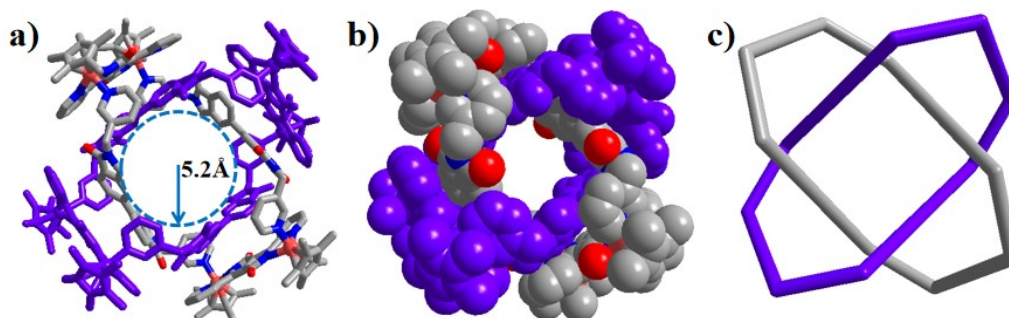


**Fig. S2** Single-crystal X-ray structure of **3**. a) Wireframe representation; b) Simplified presentation. Most hydrogen atoms, anions, solvent molecules and disordered elements are omitted for clarity.

## 4. NMR Spectra

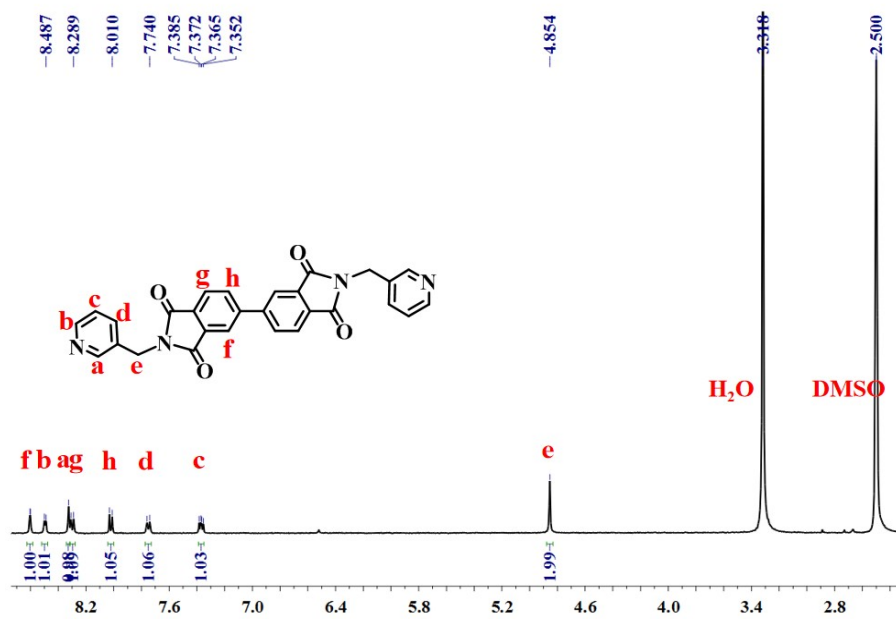


Fig. S3. The  $^1\text{H}$  NMR spectra of ligand L1 in DMSO-D6 solution.

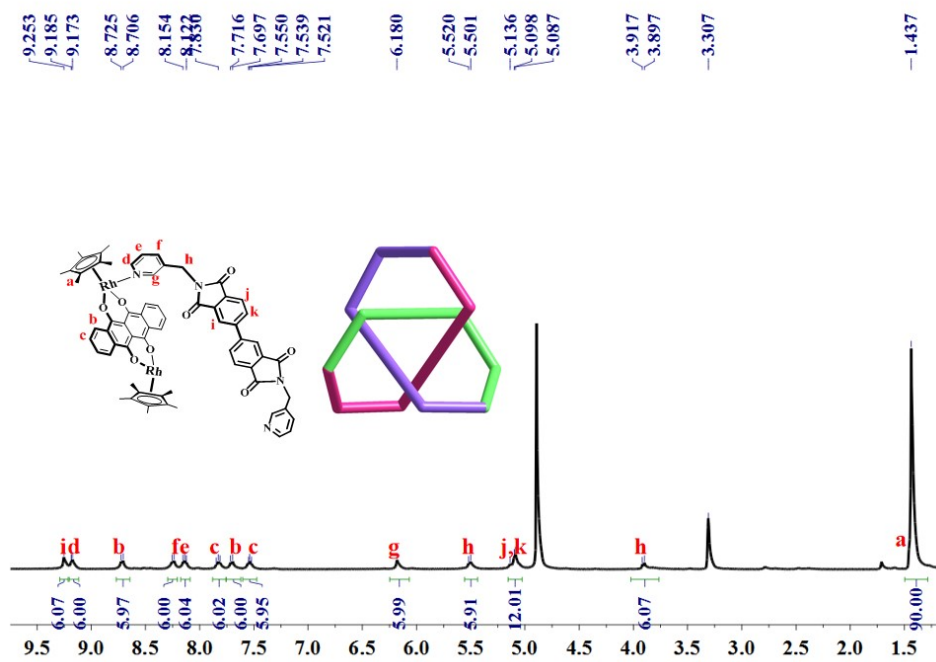
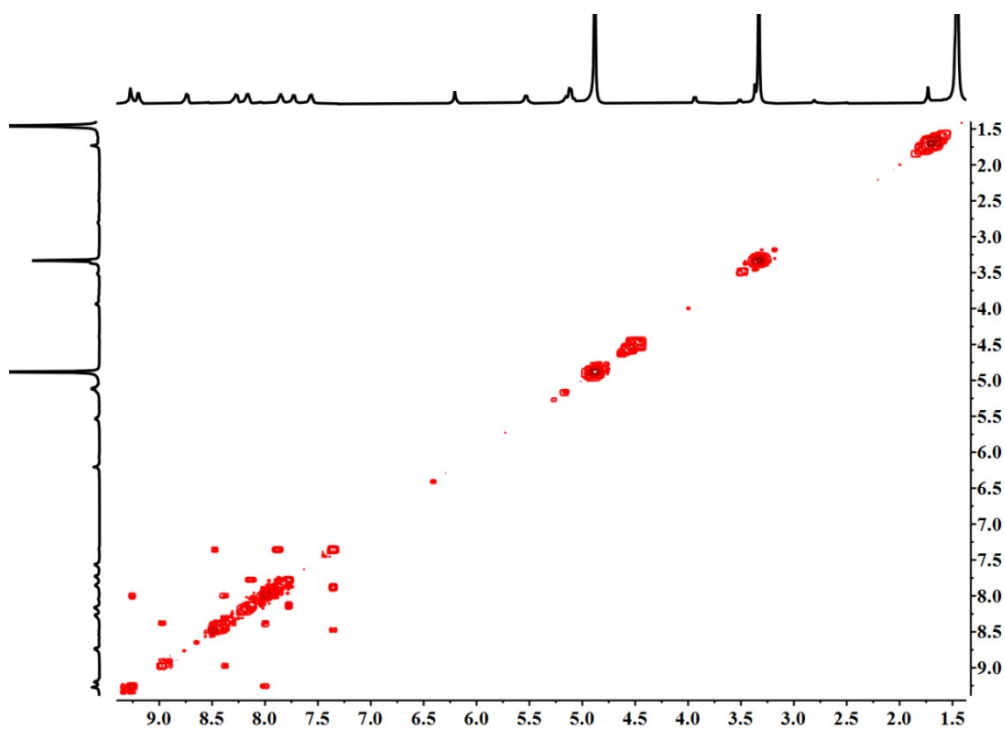
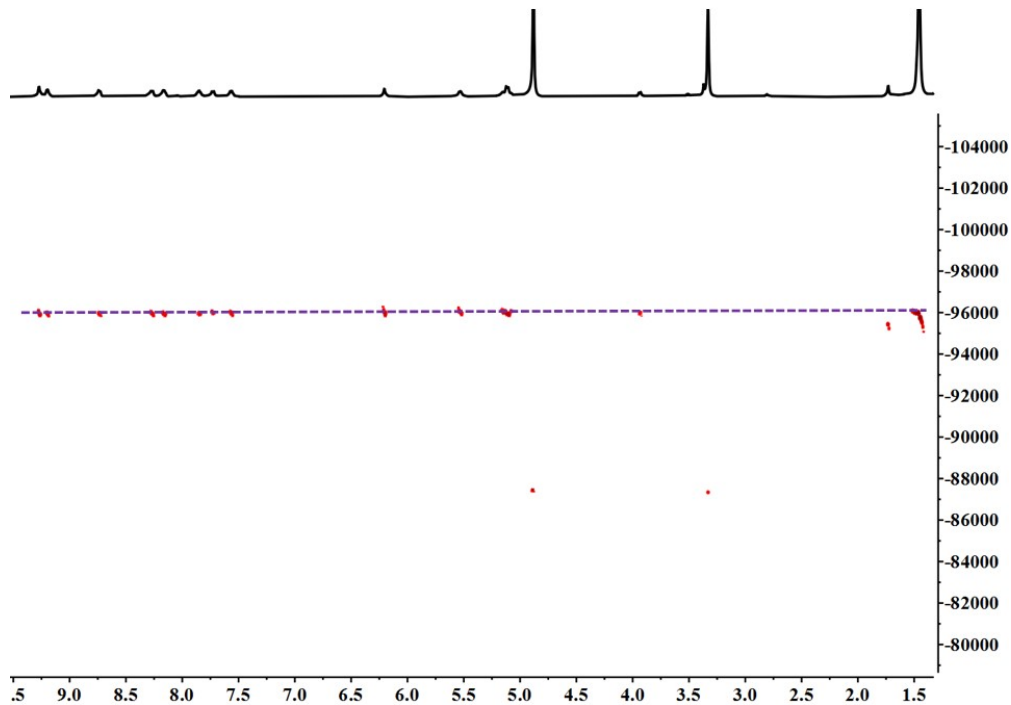


Fig. S4. The  $^1\text{H}$  NMR (500 MHz,  $\text{CD}_3\text{OD}$ , ppm) for complex 1 (15.0 mM, with respect to  $\text{Cp}^*\text{Rh}$ ).



**Fig. S5.** The <sup>1</sup>H COSY NMR (500 MHz, CD<sub>3</sub>OD, ppm) for complex **1** (15.0 mM, with respect to Cp\**Rh*).



**Fig. S6.** The <sup>1</sup>H DOSY NMR (500 MHz, CD<sub>3</sub>OD, ppm) for complex **1** (20.0 mM, with respect to Cp\**Rh*) Diffusion coefficient:  $2.0 \times 10^{-10} \text{ m}^2 \text{ s}^{-1}$ .

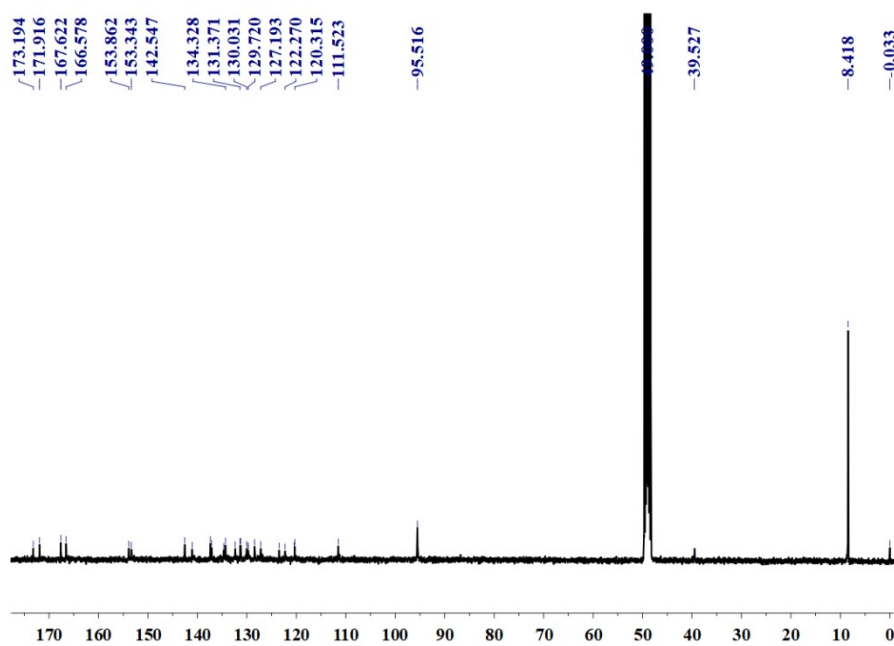


**Fig. S7.** The  $^{13}\text{C}\{^1\text{H}\}$  NMR (101 MHz,  $\text{CD}_3\text{OD}$ , ppm) for complex **1** (15.0 mM, with respect to  $\text{Cp}^*\text{Rh}$ ).

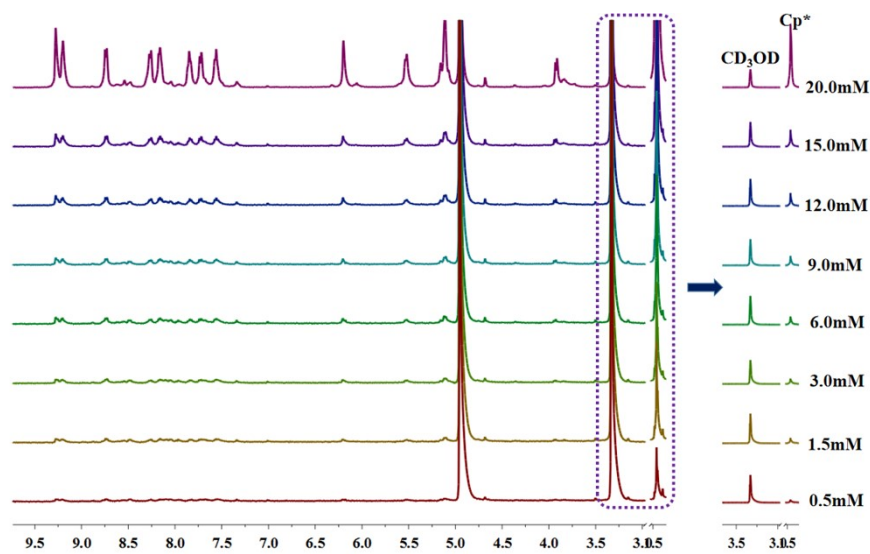


**Fig. S8.** The  $^1\text{H}$  NMR (500 MHz,  $\text{CD}_3\text{OD}$ , ppm) for trefoil knot **1** with increasing proportion of the trefoil knot **1** (0.5-20.0 mM, with respect to  $\text{Cp}^*\text{Rh}$ ).

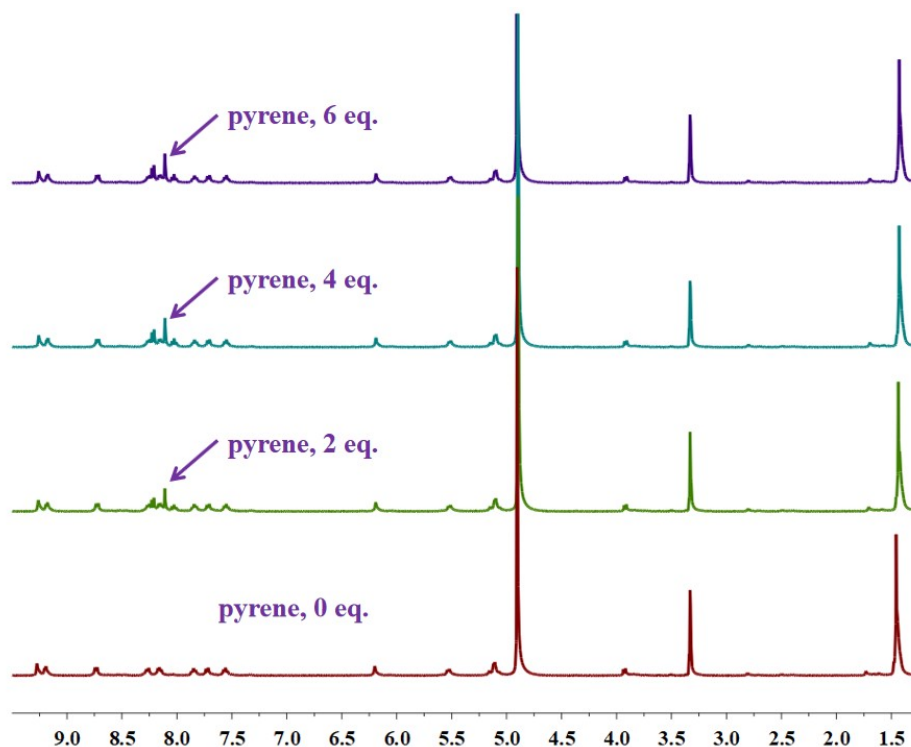


**Fig. S9.** The <sup>1</sup>H NMR (500 MHz, CD<sub>3</sub>OD, ppm) for trefoil knot **1** with increasing proportion of the trefoil knot **1** upon addition of pyrene from 0 eq. to 6 eq. (15.0 mM, with respect to Cp\*Rh).

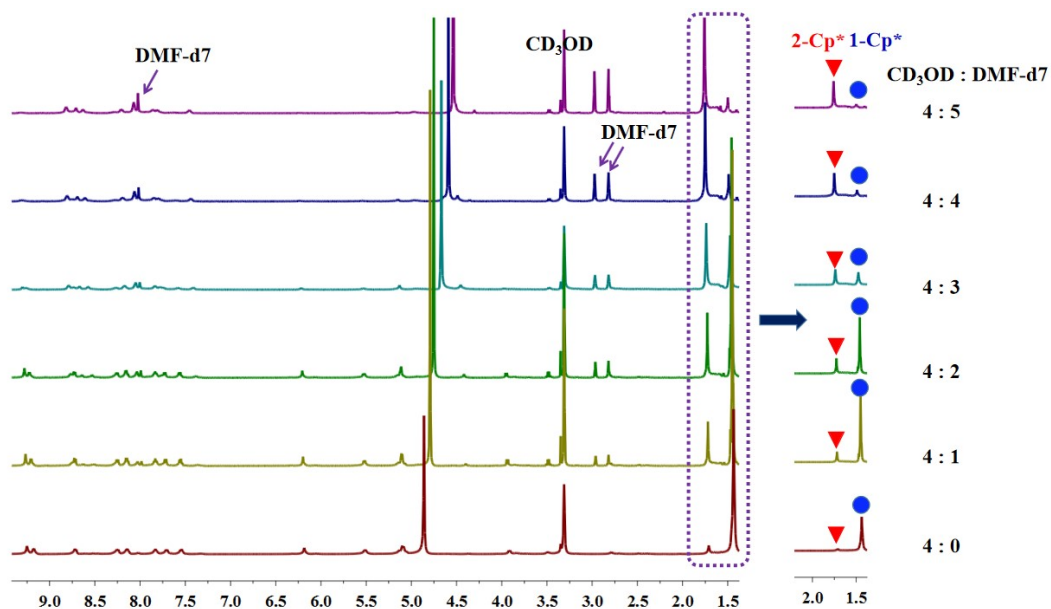


**Fig. S10.** The <sup>1</sup>H NMR spectra showing the interconversion between trefoil knot **1** and tetranuclear macrocycle **2** upon changing the solvent ratio (CD<sub>3</sub>OD/DMF [25.0 mM, with respect to Cp\*Rh], 500 MHz).

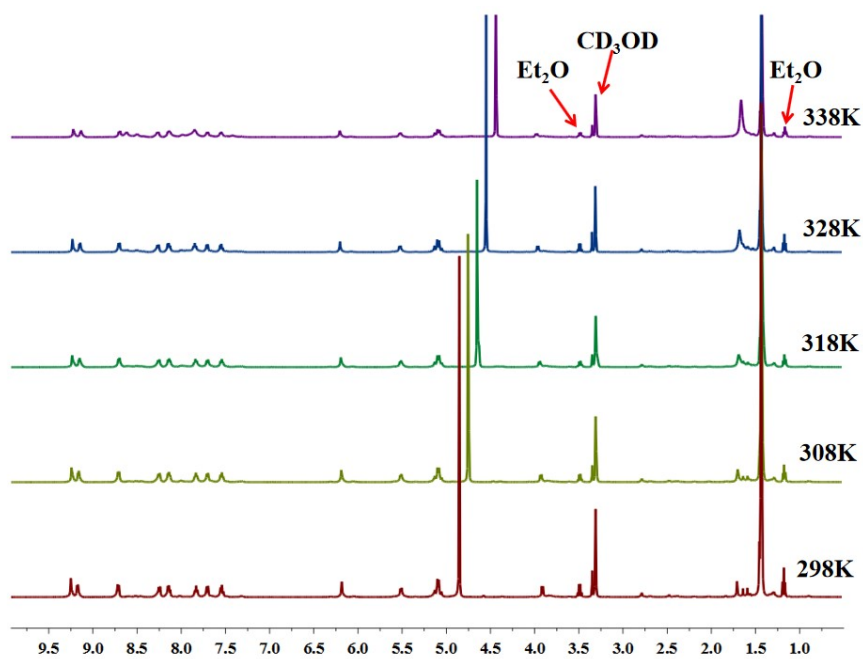


Fig. S11. Variable-temperature  $^1\text{H}$  NMR studies of complex **1** in  $\text{CD}_3\text{OD}$  solution.

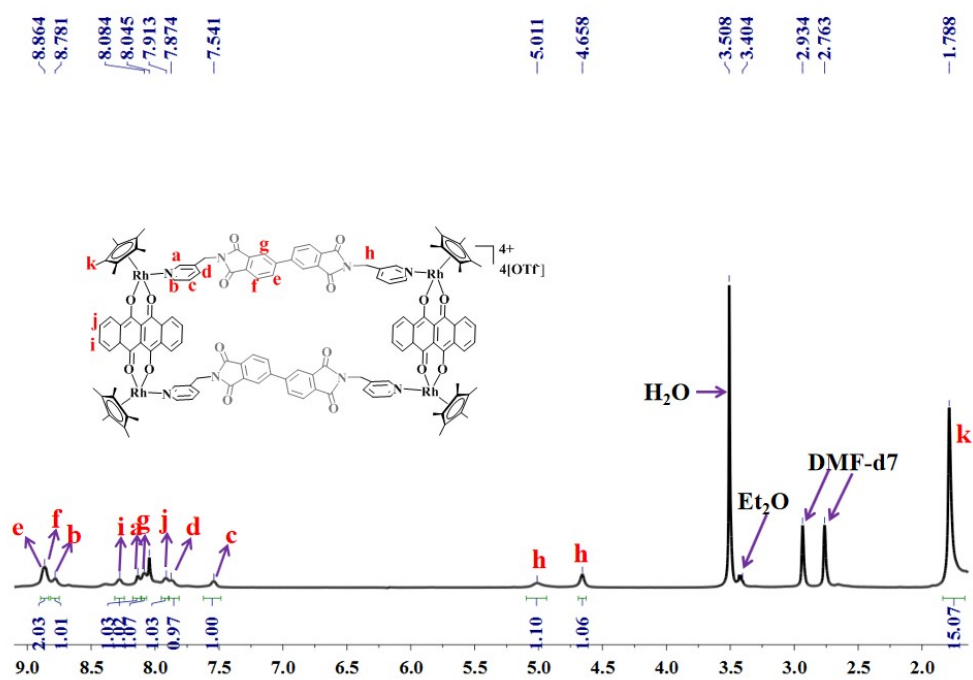
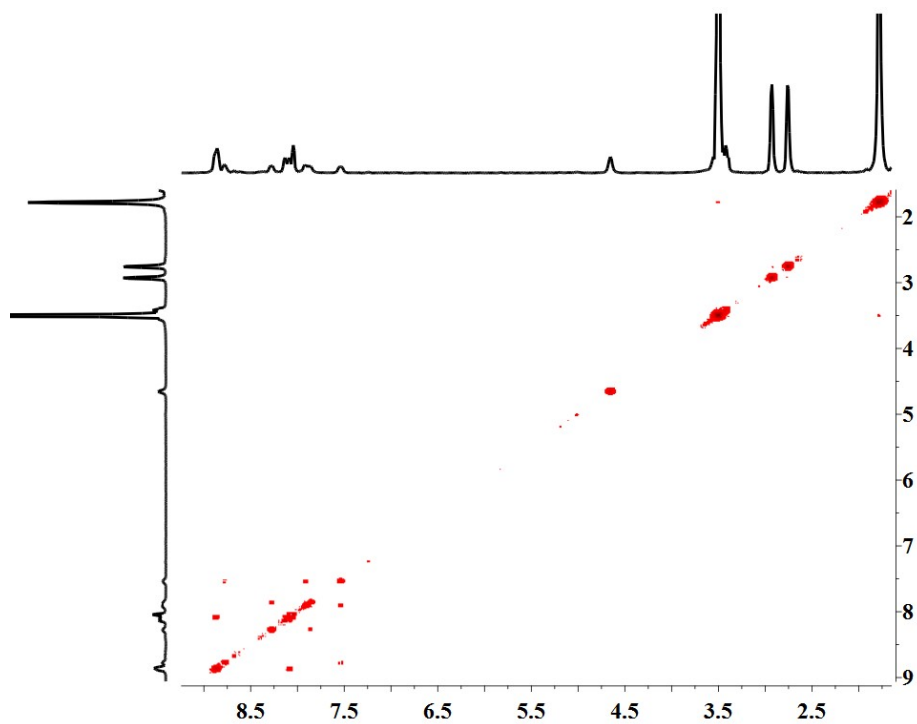
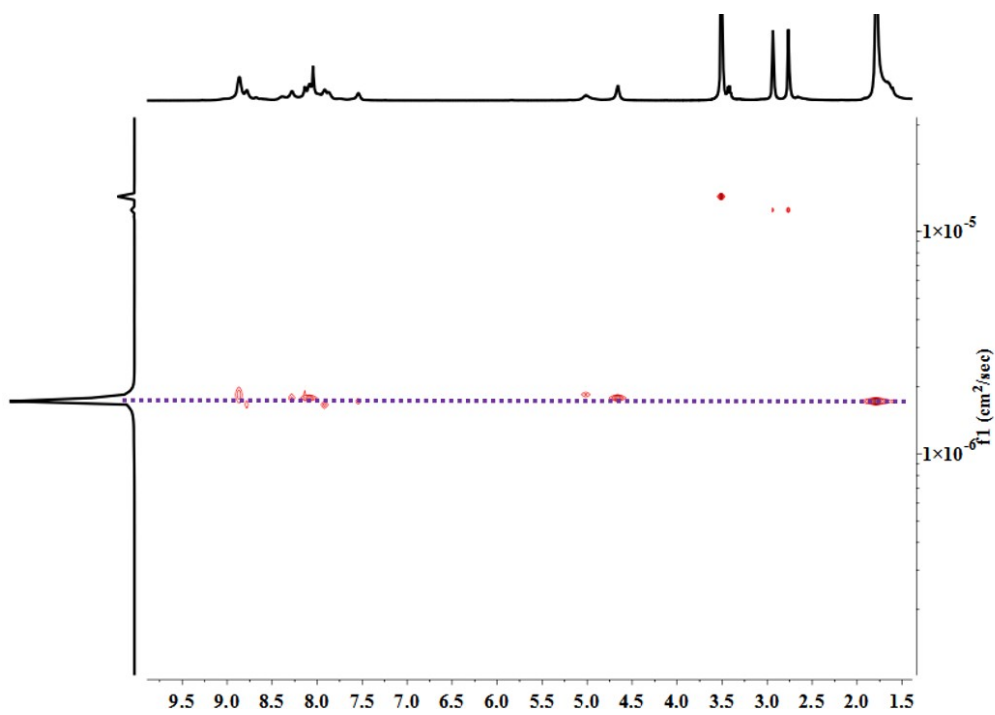


Fig. S12. The  $^1\text{H}$  NMR (500 MHz,  $\text{CD}_3\text{OD}$ , ppm) for complex **2** (24.0 mM, with respect to  $\text{Cp}^*\text{Rh}$ ).



**Fig. S13.** The  $^1\text{H}$  COSY NMR (500 MHz,  $\text{CD}_3\text{OD}$ , ppm) for complex **2** (24.0 mM, with respect to  $\text{Cp}^*\text{Rh}$ ).



**Fig. S14.** The  $^1\text{H}$  DOSY NMR (500 MHz,  $\text{CD}_3\text{OD}$ , ppm) for complex **2** (24.0 mM, with respect to  $\text{Cp}^*\text{Rh}$ ) Diffusion coefficient:  $1.7 \times 10^{-10} \text{ m}^2\text{s}^{-1}$ .

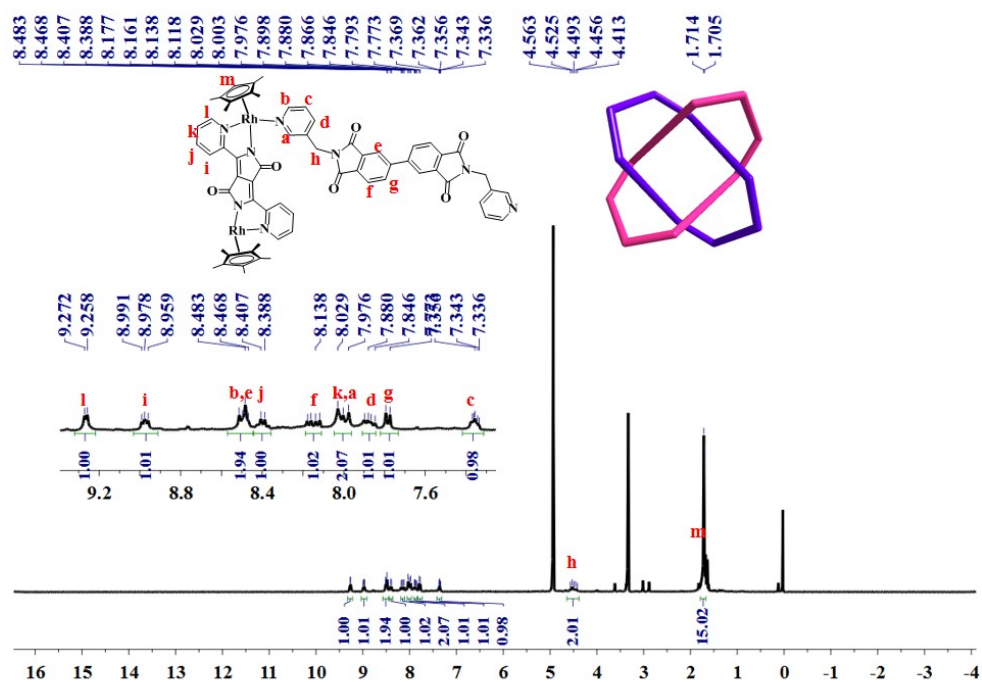


Fig. S15. The  $^1\text{H}$  NMR (500 MHz,  $\text{CD}_3\text{OD}$ , ppm) for Solomon 3 (25.0 mM, with respect to  $\text{Cp}^*\text{Rh}$ ).

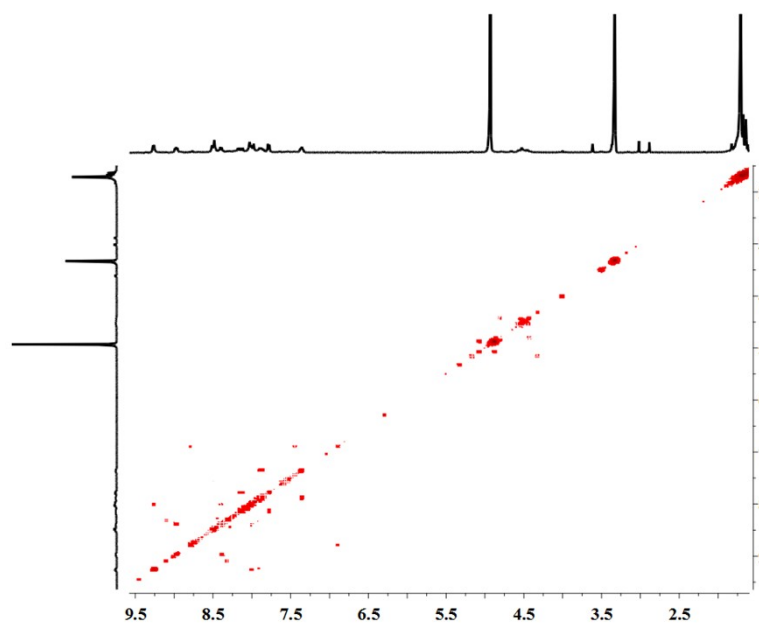
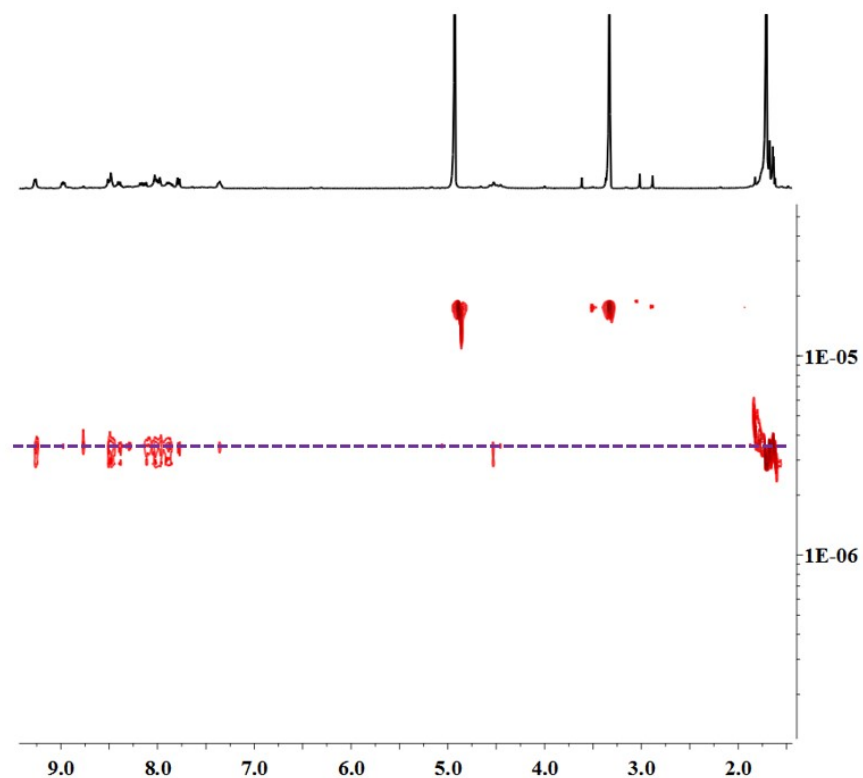
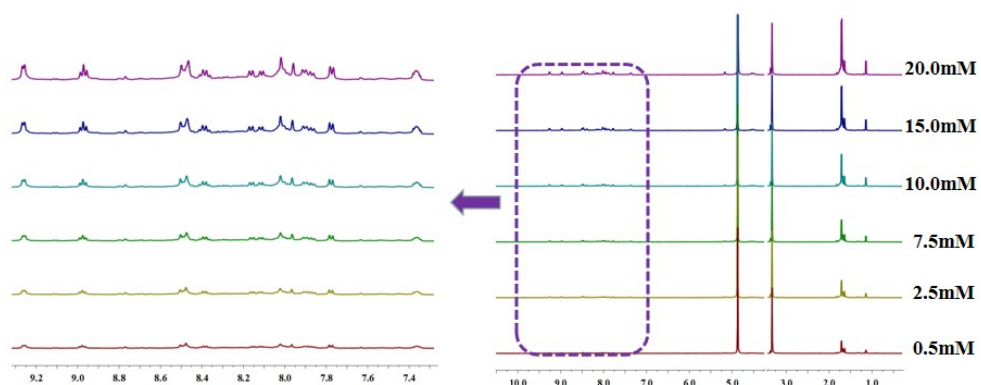


Fig. S16. The  $^1\text{H}$  COSY NMR (500 MHz,  $\text{CD}_3\text{OD}$ , ppm) for Solomon 3 (25.0 mM, with respect to  $\text{Cp}^*\text{Rh}$ ).



**Fig. S17.** The  $^1\text{H}$  DOSY NMR (500 MHz,  $\text{CD}_3\text{OD}$ , ppm) for complex **3** (20.0 mM, with respect to  $\text{Cp}^*\text{Rh}$ ) Diffusion coefficient:  $3.2 \times 10^{-10} \text{ m}^2\text{s}^{-1}$ .



**Fig. S18.** The  $^1\text{H}$  NMR (500 MHz,  $\text{CD}_3\text{OD}$ , ppm) for stable Solomon link **3** with increasing proportion of the Solomon link **3** (0.5-20.0 mM, with respect to  $\text{Cp}^*\text{Rh}$ ).

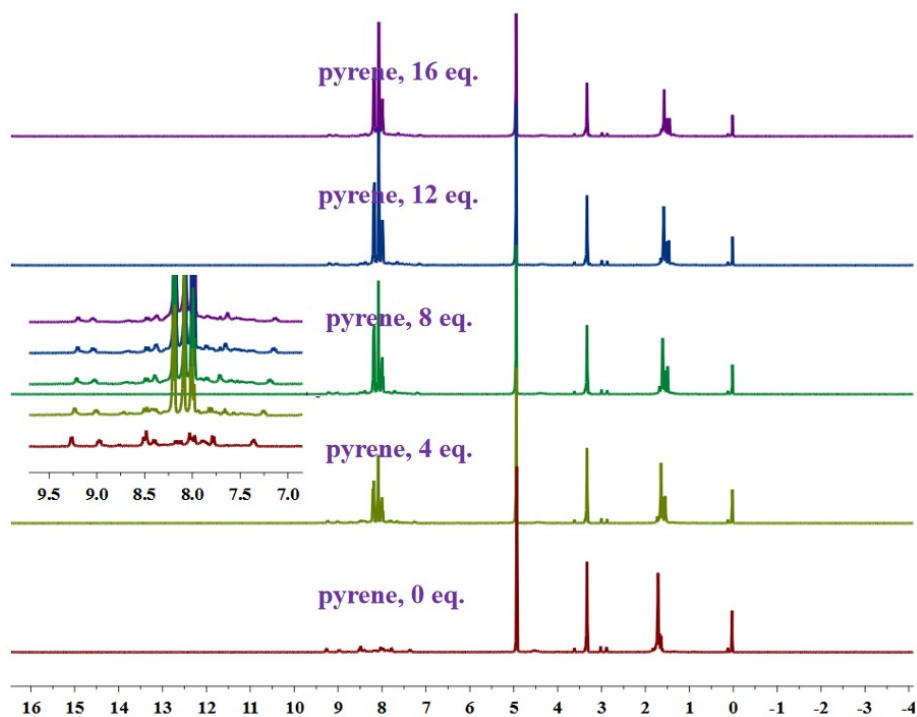


**Fig. S19.** The <sup>1</sup>H NMR (500 MHz, CD<sub>3</sub>OD, ppm) for stable Solomon link **3** with increasing proportion of the Solomon link **3** upon addition of pyrene from 0 eq. to 16 eq. (25.0 mM, with respect to Cp\*Rh).

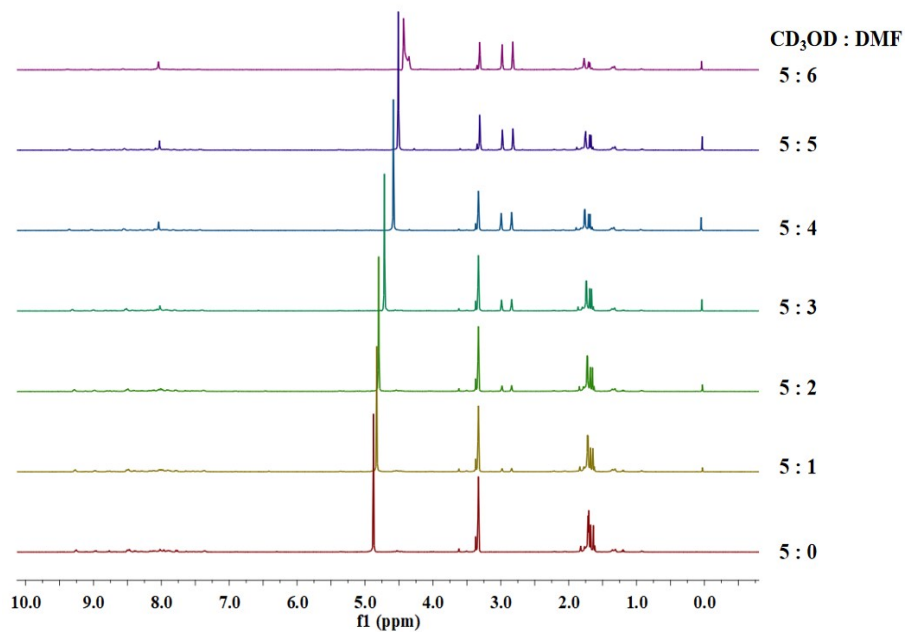


**Fig. S20.** The <sup>1</sup>H NMR spectra showing the stable structure of the Solomon link **3** despite changing the solvent ratio (CD<sub>3</sub>OD/DMF [25.0 mM, with respect to Cp\*Rh], 500 MHz).

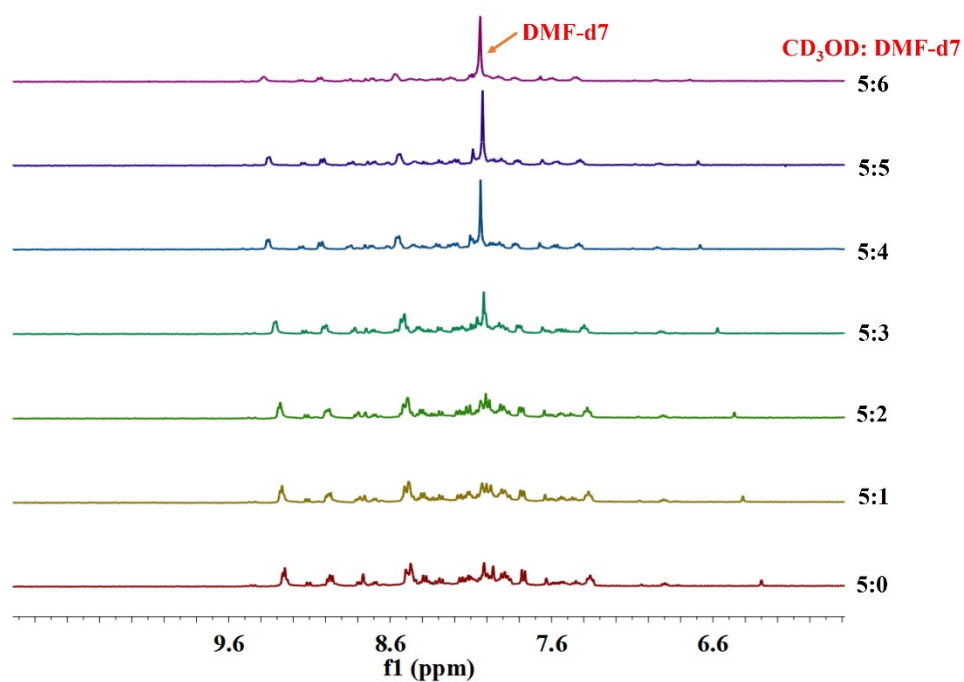


**Fig. S21.** The partial <sup>1</sup>H NMR spectra showing the stable structure of the Solomon link **3** despite changing the solvent ratio (CD<sub>3</sub>OD/DMF [23.0 mM, with respect to Cp\*Rh], 500 MHz).

## 5. UV-vis-NIR absorption spectra

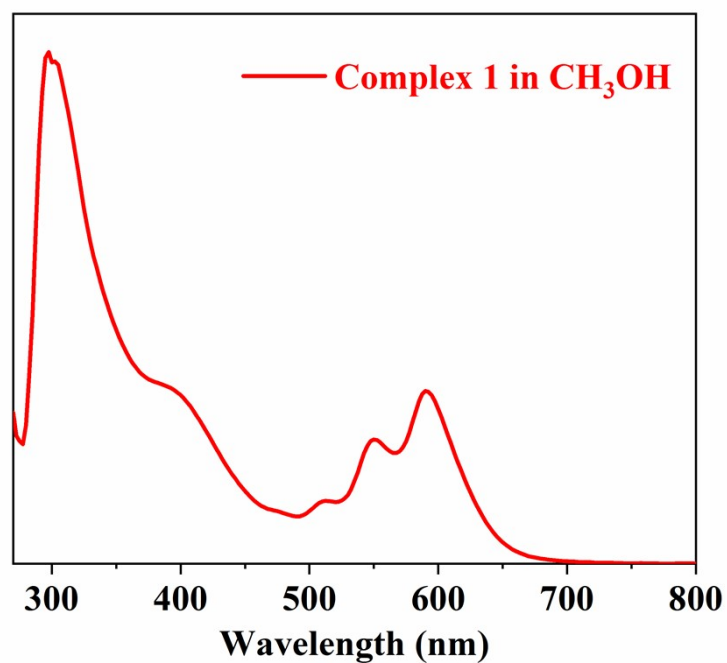


**Fig. S22.** UV-vis-NIR absorption spectra of trefoil knot **1** (methanol,  $c = 10^{-5}$  M,  $T = 300$  K).

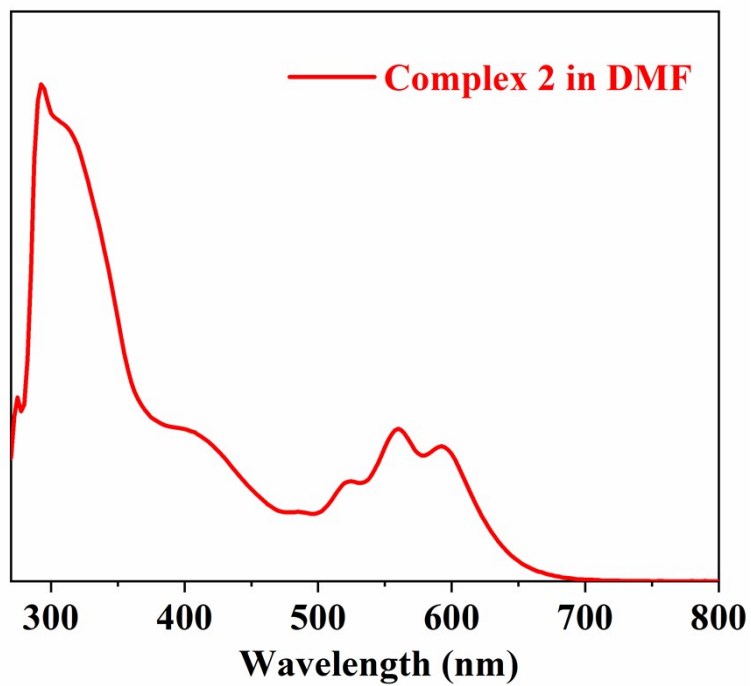


**Fig. S23.** UV-vis-NIR absorption spectra of [2+2] macrocycle **2** (N, N-Dimethylformamide,  $c = 10^{-5}$  M,  $T = 300$  K).

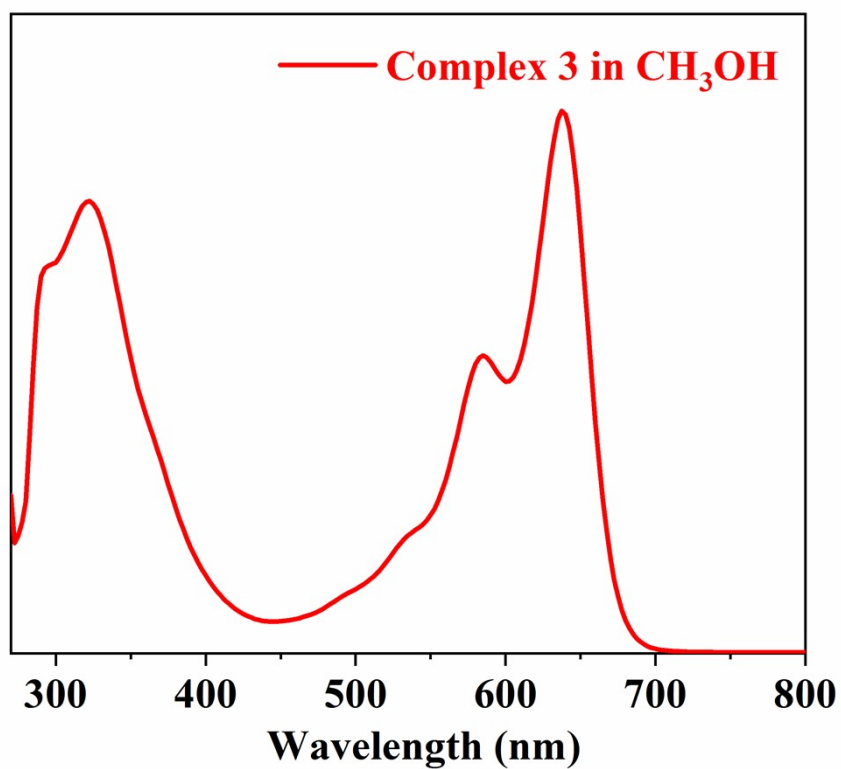


**Fig. S24.** UV-vis-NIR absorption spectra of Solomon **3** (methanol,  $c = 10^{-5}$  M,  $T = 300$  K).

## 6. ESI-MS spectra

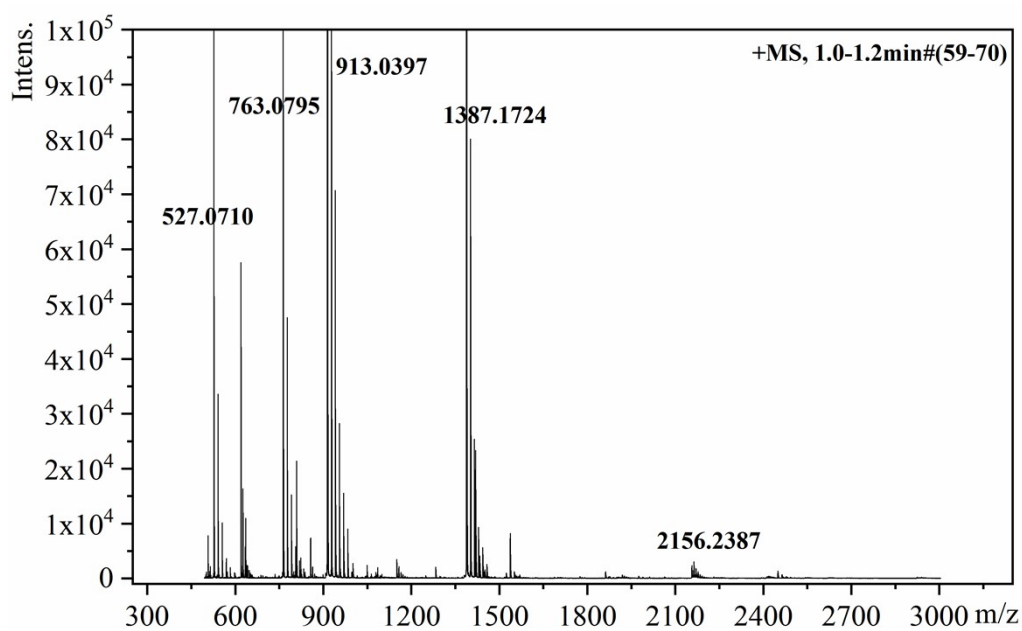


**Fig. S25.** Full ESI-MS spectra of **1**, the prominent signal at  $m/z = 2156.23$  for  $[1-2OTf]^{2+}$ .

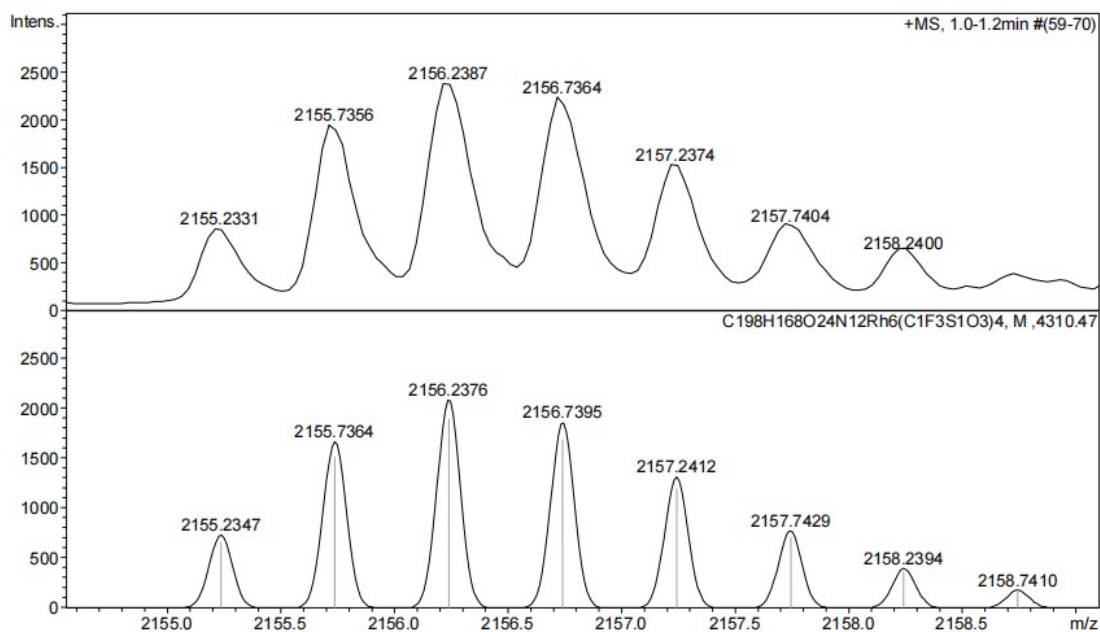


**Fig. S26.** Experimental (top) and theoretical (bottom) ESI-MS spectra of  $[1-2OTf]^{2+}$ .

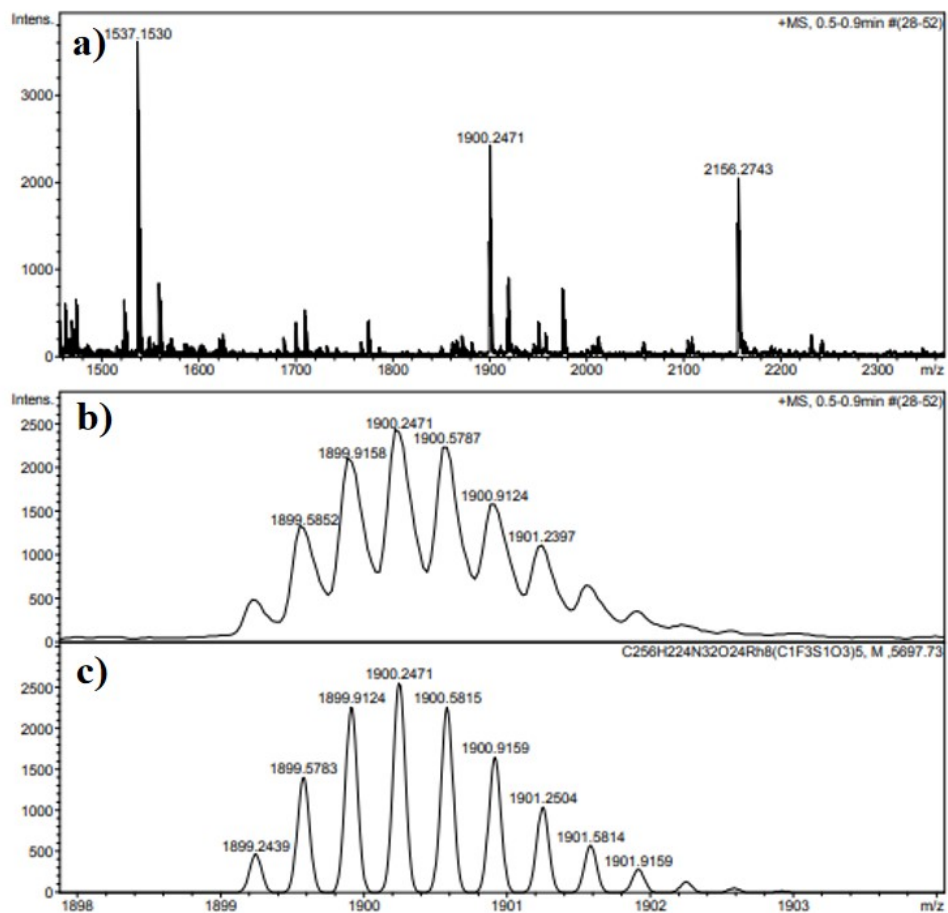


**Fig. S27.** Full ESI-MS spectra (a) of complex 3, experimental (b) and theoretical (c) ESI-MS spectra of  $[3 - 3OTf]^{3+}$ .

## 7.DFT computational details

The density functional theory (DFT) calculations were performed by using the Vienna Ab initio Simulation Package (VASP) code with the projector augmented wave (PAW) method.<sup>[2,3]</sup> The exchange-functional was treated using the generalized gradient approximation (GGA) of Perdew-Burke-Ernzerhof (PBE) functional.<sup>[4]</sup> Wave functions were expanded using a plane-wave basis set with kinetic energy cutoff of 400 eV and the geometries were fully relaxed until the residual force convergence value on each atom being less 0.05 eV/Å. The Brillouin zone integration was performed using 2×2×2 Monkhorst-Pack k-point sampling for a primitive cell.<sup>[5]</sup> The self-consistent calculations applied a convergence energy threshold of 10<sup>-4</sup> eV. Spin-polarization was considered in all calculations.<sup>[6]</sup>

**Table S1.** Energetic results for the formation of a Solomon link from 4 ligands **L1** and 4 building blocks **E2** and for the formation of a [2+2] macrocycle from 2 ligands **L1** and 2 building blocks **E2**. Energy comparison (Same number of atoms): Solomon link = [2+2] macrocycle × 2:

	Solomon link <b>3</b>	monocycle <b>3'</b>
Energy	-3614.24	-1806.49
Total Energy (Same number of atoms)/eV	-3614.24	-3612.98

Density functional theory (DFT) calculations shows that Solomon link **3** has lower energy than two non-interlocked [2+2] macrocycle **3'**, proving that the doubly-interlocked topology, Solomon link **3**, is easier to form and has higher stability than non-interlocked [2+2] macrocycle **3'**.

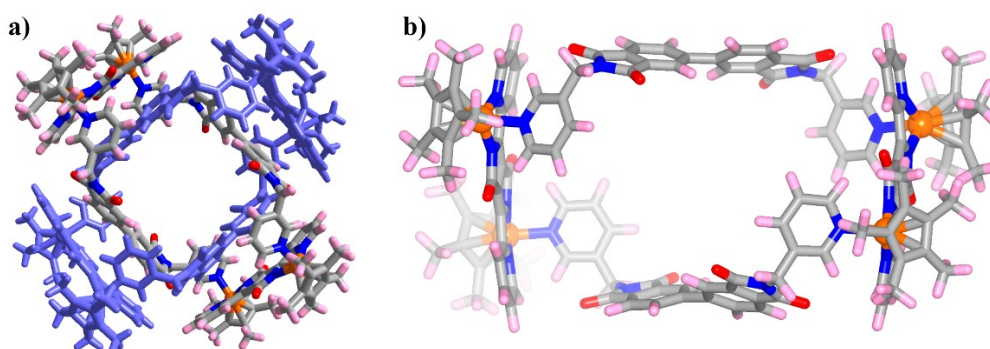


**Fig. S28.** The optimized geometries of Solomon link **3** and [2+2] macrocycle **3'**.

## 8.X-ray crystallography details

Single crystals suitable for X-ray diffraction studies were obtained by recrystallization at room temperature. X-ray intensity data of **1** and **3** were collected on a CCD-Bruker SMART APEX diffractometer at 173 K. Disordered solvent molecules that could not be restrained properly were removed using the SQUEEZE routine in all data sets. Crystal data collection and refinement parameters of the X-ray diffraction studies are listed in Tables S2-S3.

In asymmetric unit of **1**, A solvent mask was calculated and 1115 electrons were found in a volume of 3056 Å<sup>3</sup> in 2 voids per unit cell. This is consistent with the presence of 9[C<sub>6</sub>H<sub>14</sub>O], 1[CH<sub>3</sub>OH] per Asymmetric Unit which account for 1080 electrons per unit cell.

**Table S2. Crystal data and structure refinement for complex 1**

Empirical formula	C <sub>224</sub> H <sub>236</sub> F <sub>18</sub> N <sub>12</sub> O <sub>56</sub> Rh <sub>6</sub> S <sub>6</sub>	
Formula weight	5144.05	
Temperature	173(2) K	
Wavelength	1.34138 Å	
Crystal system	Triclinic	
Space group	P-1	
Unit cell dimensions	a = 16.554(3) Å	α = 86.260(7)°.
	b = 21.628(3) Å	β = 85.845(7)°.
	c = 31.264(5) Å	γ = 82.804(7)°.
Volume	11059(3) Å <sup>3</sup>	
Z	2	
Density (calculated)	1.545 Mg/m <sup>3</sup>	
Absorption coefficient	3.296 mm <sup>-1</sup>	
F(000)	5280	
Crystal size	0.420 x 0.190 x 0.130 mm <sup>3</sup>	
Theta range for data collection	2.933 to 55.063°.	
Index ranges	-20 ≤ h ≤ 20, -26 ≤ k ≤ 26, -38 ≤ l ≤ 36	
Reflections collected	145459	
Independent reflections	42011 [R(int) = 0.0548]	
Completeness to theta = 53.594°	99.8 %	
Absorption correction	Semi-empirical from equivalents	
Max. and min. transmission	0.751 and 0.421	
Refinement method	Full-matrix least-squares on F <sup>2</sup>	
Data / restraints / parameters	42011 / 1256 / 2901	
Goodness-of-fit on F <sup>2</sup>	1.019	
Final R indices [I > 2σ(I)]	R1 = 0.0757, wR2 = 0.2204	
R indices (all data)	R1 = 0.0871, wR2 = 0.2306	
Extinction coefficient	n/a	
Largest diff. peak and hole	2.442 and -1.363 e.Å <sup>-3</sup>	

**Table S3. Crystal data and structure refinement for complex 3**

Empirical formula	C <sub>240</sub> H <sub>364</sub> F <sub>12</sub> N <sub>16</sub> S <sub>4</sub> O <sub>42</sub> Rh <sub>4</sub>	
Formula weight	4910.18	
Temperature	173.0 K	
Wavelength	1.54178 Å	
Crystal system	Tetragonal	
Space group	P4/mnc	
Unit cell dimensions	a = 33.6939(16) Å	α = 90°.
	b = 33.6939(16) Å	β = 90°.
	c = 34.994(3) Å	γ = 90°.
Volume	39728(5) Å <sup>3</sup>	
Z	8	
Density (calculated)	1.444 Mg/m <sup>3</sup>	
Absorption coefficient	3.273 mm <sup>-1</sup>	
F(000)	18496	
Crystal size	0.11 x 0.1 x 0.04 mm <sup>3</sup>	
Theta range for data collection	1.820 to 24.999°.	
Index ranges	-18 ≤ h ≤ 18, -18 ≤ k ≤ 18, -19 ≤ l ≤ 19	
Reflections collected	30607	
Independent reflections	1792 [R(int) = 0.1294]	
Completeness to theta = 24.999°	99.7 %	
Absorption correction	Semi-empirical from equivalents	
Max. and min. transmission	0.891 and 0.736	
Refinement method	Full-matrix least-squares on F <sup>2</sup>	
Data / restraints / parameters	1792 / 2679 / 644	
Goodness-of-fit on F <sup>2</sup>	1.122	
Final R indices [I > 2σ(I)]	R1 = 0.1471, wR2 = 0.3174	
R indices (all data)	R1 = 0.1614, wR2 = 0.3227	
Extinction coefficient	0.000112(14)	
Largest diff. peak and hole	0.532 and -0.394 e.Å <sup>-3</sup>	
CCDC	2070965	

## 9. References

1. C. White, A. Yates and P. M. Maitlis,  $\eta^5$ -Pentamethylcyclopentadienyl) rhodium and -iridium compounds. *Inorg. Synth.*, **1992**, 29, 228–234.
2. J. P. Perdew, K. Burke, M. Ernzerhof. *Physical review letters.*, **1996**, 77, 3865.
3. G. Kresse, D. Joubert. *Physical Review B.*, **1999**, 59, 1758.
4. H. Kim, K. Lee, S. I. Woo, Y. Jung. *Phys. Chem. Chem. Phys.*, **2011**, 13, 17505-17510.
5. L. Gong, D. Zhang, C.-Y. Lin, Y. Zhu, Y. Shen, J. Zhang, X. Han, L. Zhang, Z. Xia. *Adv. Energy Mater.* **2019**, 9, 1902625.
6. L. Gong, D. Zhang, Y. Shen, X. Wang, J. Zhang, X. Han, L. Zhang, Z. Xia. *Journal of Catalysis.* **2020**, 390, 126-134.